Proceedings of The Canadian Society for Mechanical Engineering International Congress 2012
CSME International Congress 2012
June 4-6, 2012, Winnipeg, Manitoba, Canada

ATLAS MOTION PLATFORM: FULL-SCALE PROTOTYPE

M. John D. Hayes, Robert G. Langlois
Department of Mechanical and Aerospace Engineering
Carleton University
Ottawa, ON., Canada

Abstract— Conventional training simulators commonly use the hexapod configuration to provide motion cues. While widely used, studies have shown that hexapods are incapable of producing the range of motion required to achieve *high fidelity* simulation required in many applications. This paper presents an overview of the design of the first full-scale prototype of the Atlas motion platform. The Atlas concept was introduced in 2005, and is unique in that orienting is decoupled from positioning, and unlimited rotations are possible about any axis of the mechanism. The key to the design is three mecanum wheels in an equilateral arrangement, which impart angular displacements to a sphere that houses the cockpit, thereby providing rotational actuation. Since the Atlas sphere rests on these mecanum wheels, there are no joints or levers constraining its motion, allowing full 360° motion about all axes, yielding an unbounded orientation workspace that is singularity free. In this paper, high-level design details regarding actuation, the spherical shell, and the system infrastructure that will provide the pilot with a realistic and high fidelity simulation are described.

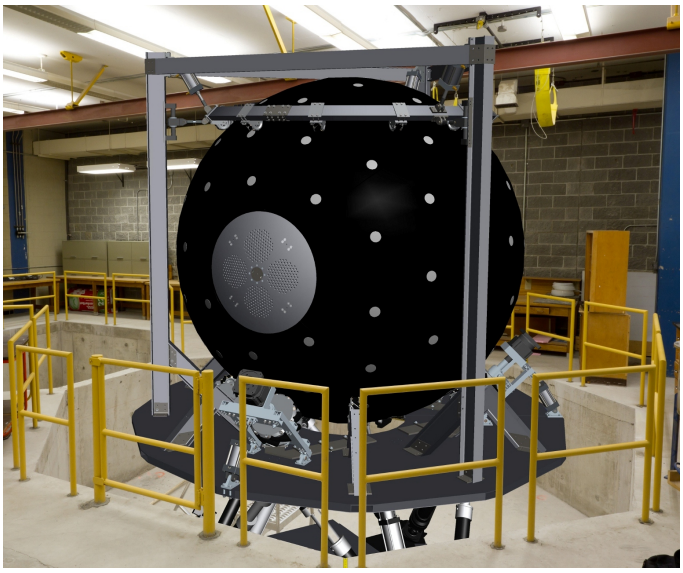

Figure 1. A 3D Rendering of the Atlas Simulator.

I. INTRODUCTION

Since its inception in 2002, the Carleton University Simulator Project (CUSP), a fourth year capstone design project, has incrementally advanced the development of a novel simulator system that overcomes motion limitations associated with industry-standard simulator motion platforms based on hexapods. The full-scale design is called the *Atlas simulator motion platform* and is illustrated in Figure 1. The unique design of Atlas decouples its three-dimensional translational workspace from its unbounded, singularity free orientation workspace [1]. In the proposed configuration, a Gough-Stewart platform [2, 3] is used to provide translation while Atlas provides the rotation.

The concept of spherical actuation is not new. Spherical dc induction motors were introduced in 1959 [4]. Developments continued over the next 30 years leading to designs presented in [5] and [6], for example. However, due to physical limitations imposed by the stator and commutator, angular displacements are limited. Unbounded rotational motion is achieved by the Eclipse II architecture [7], however its orientation workspace is constrained by structural interferences, and rotation limits of the spherical joints. Further, there is no closed form algebraic model for its kinematics and the velocity level kinematics require estimating parameters numerically. The Desdemona motion platform [8] uses a fully gimballed system to allow for rotation about any axis. Its range of motion allows up to 8 m of horizontal translation, and 2 m of vertical displacement. However, because of the gimbal arrangement, the orientation workspace is not free of singularities because of the potential of gimbal-lock.

The unique features, capabilities, and requirements of Atlas have necessitated the development of a number of core technologies, including the mechanical design of the mecanum wheel actuation system, sphere orientation sensing, sphere orientation control, a distributed simulation architecture, fabrication methods, unique test methods, as well as a variety of safety systems and procedures. These various technologies have progressed through numerous design iterations and refinements. In particular, the rotational actuation concept has been demonstrated with the AtlasLite demonstrator [9] using omni-wheels and an 8 inch

diameter sphere, and the Technology Demonstrator Platform (TDP) [10] using mecanum wheels and a 1.37 m (4.5 ft) diameter sphere. AtlasLite has continued to serve as the main platform for advancing the visual orientation system (VOS) as well as sensor fusion approaches with the inertial orientation system (IOS). The TDP has enabled exploring sphere manufacturing techniques using composites, actuation using a variety of driving wheel designs, and realization of the Real Time Platform (RTP) control architecture.

Please note that the use of dual metric and Imperial dimensioning reflects the reality of design in Canada: the standard is metric, however many stock components are sized in Imperial units. The full scale Atlas prototype comprises three major systems: the actuation system; the sphere structure; and the simulation system. The actuation system involves the Gough-Stewart platform, sphere support structure, and rotational actuation system. The sphere structure comprises the spherical cockpit shell, internal support structure, and two hatches with a nested ventilation system. Finally, the simulation system consists of the distributed computing architecture, real time platform, vehicle models, user interface devices, internal sphere power system, and cockpit components.

II. Actuation

A. *Translation*

Figure 2. Moog MB-EP-6DOF 2800KG motion platform.

The motion base that has been selected to provide the translational motion requirements of the Atlas prototype is a Moog MB-EP-6DOF 2800KG Gough-Stewart hexapod. The platform has a payload capacity of 2800 kg, and the estimated total weight of the upper Atlas platform is less than 1400 kg. This component has been purchased and installed in the Atlas lab. This option was selected due to the prohibitive cost of an adequately sized gantry system.

Since a hexapod is a six-degree-of-freedom (DoF) actuator, it provides capability for rotational as well as translational motion. This rotational motion will be constrained to limit the motion of the platform to be strictly translational using the software controls of the platform. The platform is illustrated in Figure 2. The Moog MB-EP-6DOF 2800KG has a maximum displacement of $\pm$ 0.57 m (22.4 in) surge, $\pm$ 0.49 m (19.3 in) sway, $\pm$ 0.39 m (15.4 in) heave. The motion base is secured to the floor using twelve 24 mm diameter Hilti bolts anchored in a 500 mm thick pad of concrete to ensure that the assembly is properly supported.

Analysis was performed on the platform to understand both the workspace of the system and the dynamics of the actuators. This will aid in determining the performance characteristics as well as ensure safe operation of the prototype. Software tools were created in order to allow specific situations to be analyzed.

B. *Orientation*

Three active mecanum wheels are used to change the sphere orientation. These wheels offer suitable load carrying capacity and can provide omnidirectional rotation of the sphere while introducing minimal vibration. Developing mecanum wheels in-house allowed the weight to be reduced by half and the cost to be reduced by two thirds compared to comparable commercially-available wheels. It also allowed for control over the characteristics of the interface between the mecanum wheels and the sphere surface. Urethane roller material and finish has been selected to provide a contact patch of approximately 50 mm^2 (2 in^2) and a minimum coefficient of friction of 0.6. Moreover, the roller profiles are elliptical thereby enhancing the transition between rollers as the mecanum wheel rotates, further reducing vibration.

In addition to the active mecanum wheels, two rings of smaller passive mecanum wheels, each containing 12 passive wheels, will be used to help constrain translation of the sphere relative to the support structure, and to ensure sufficient normal force at the contact patch to prevent slip in the driving direction. Detailed design drawings of both the passive and driving wheels have been completed. A solid rendering of one of the active wheels is illustrated in Figure 3.

Figure 3. Driving mecanum wheel design.

To ensure all contact points between the 24 passive and three active mecanum wheels and the surface of the Atlas sphere would experience contact pressure sufficiently less than the yield strength of the sphere, computational algorithms were developed to determine the loads at all these contact points.

The first algorithm allows for the simultaneous calculation of the highest wheel torque, tractive force, and normal force that any of the driven mecanum wheels would experience under specified angular acceleration. The algorithm uses Euler's equation of motion to find the maximum torque experienced by the sphere, and then uses a Jacobian relation to compute the corresponding maximum wheel torque, which also corresponds to the maximum normal force. The algorithm then determines the normal force required to attain the performance requirements. The results are listed in Table I. Once accurate estimates of the sphere composite properties are known, these results will define the maximum angular acceleration.

TABLE I. Loading results.

Accel	Max Wheel Torque	Normal (lb)		
$(^\circ/s^2)$	$(lb \cdot in)$	$\mu = 0.6$	$\mu = 0.65$	$\mu = 0.7$
300	2850	900	835	780
320	3015	950	880	820
340	3205	1010	935	870
360	3400	1070	990	920
400	3770	1190	1100	1025
450	4250	1340	1240	1155
500	4710	1485	1375	1280
550	5200	1640	1515	1410
600	5660	1780	1645	1530
650	6125	1940	1780	1655

The second algorithm simulates inertial loading to establish the loads on each castor wheel that results in dynamic equilibrium between the sphere surface and contact patches. Iterating through different loading conditions, the algorithm computed the highest magnitude of normal force that any castor wheel will experience. For the maximum linear acceleration of 0.8 g generated by the Moog platform, the results are listed in Table II.

TABLE II. Results from castor wheel simulation.

Maximum Normal Force Top (lb)	240
Maximum Normal Force Bottom (lb)	212

C. *Motors and Mounting*

The active mecanum wheel mounts are required to support the mecanum wheel and motor assembly while supplying a controllable amount of force to the Atlas sphere at an accurate angle and orientation. To do this, the lower mount uses a pneumatic suspension system which rotates the mecanum wheel and motor assembly about a fixed axis towards its contact point. The rotation is produced by a pneumatic actuator positioned at the motor end of the assembly. Since the displacement is very small, the contact angle is essentially constant. The gear box is connected to the mecanum wheel using a low alloy, high strength steel drive shaft. Using a rigid clamp coupler the drive shaft is connected to the gearbox output. The maximum torque required per mecanum wheel to satisfy the design parameter is 600 N-m (443 lbf-ft) and the maximum angular speed required per wheel is 270°/s. By analyzing the various components of the system under the given applied force and output torque, the stress in each component was determined. The required motor torque and speed, gear box ratio, and gear box output speed was calculated to select the appropriate motors and gearboxes.

In order to withstand the bending and torsion loads caused by the normal forces acting on the mecanum wheels, a drive shaft of at least 32 mm (1.25 in) diameter made of SAE 4130 low alloy steel was selected due to its high ductility and strength. This allows the drive shaft to be strong yet have adequate resistance to fatigue. The drive shaft is supported by two high load pillow block bearings which are mounted to the frame box beam members.

The frame members are fabricated out of aluminum box beams and fastened together using 1/2 in bolts. Three Kollmorgen AKM AKM64L-ANCNC-00 motors are selected with a nominal torque output of 12 N-m (120 lbf-in) and a rated speed of 3500 rpm which operate at 480 VDC at a continuous current of 12A. A relatively higher voltage was selected to reduce the current requirements which would then reduce the complexity and the cost of the electronic components to drive the motors. The motors were selected taking into account a safety factor of 1.15. An Apex dynamics gear box AF180-060-S2-P2 with a 60:1 gear box reduction, rated torque of 1100 N-m (9750 lbf-in) and speed of 3000 rpm has also been selected.

D. *Support Structure*

The Atlas upper support structure design consists of three vertical I beams upon which pneumatic cylinders are mounted, see Figure 4. These cylinders apply a supplementary load to an aluminum ring onto which 12 passive mecanum wheels are mounted. A horizontal control linkage is used to constrain the ring. The ring itself maintains sufficient contact between the sphere and driving mecanum wheels. The constraining load applied by the cylinders is dependent on the input cylinder pressure controlled by the pneumatic control system. This system allows for a constant applied force regardless of motion induced variation. The pneumatic system is also equipped with default position port closed valves that will lock the cylinder pressure in the event of power loss or an air leak. To contain the sphere during total system failure, the cylinder travel is limited to 51 mm in both directions from the neutral position.

The lower support structure comprises 6 I-beam assemblies onto which 12 passive mecanum wheels, identical to those used on the upper support ring, that support the sphere during motion and allow for a constant drive system normal force. These mecanum wheels are rigidly mounted to the Moog platform so

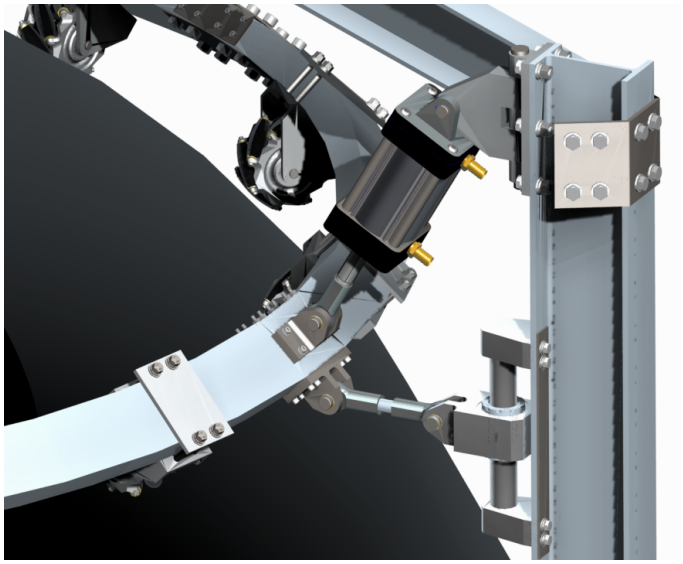

Figure 4. Upper support structure.

as to maintain a constant geometric centre. The wheels for the upper and lower support structures are interchangeable.

The motion base interface comprises radially-symmetric upper and lower structures covered with a skin of segmented aluminum plates. This design achieves objectives of lightness, stiffness, modularity, ease of manufacture, and ready access to fasteners. The structural members are aligned with the components that are mounted on the motion base interface. This alignment is crucial for stiffness and strength. For cost, simplicity, and maintenance considerations, the support structure is designed using standard fasteners and standard stock material for the manufactured components. Off-the-shelf components are also chosen wherever possible.

Structural analysis was performed on the upper support structure for deflections and stresses. The selected cylinders of 4 in diameters are able to apply a load of 1500 lbf when operating at 125 psi. A load of 1500 lbf is sufficient for the required performance characteristics of the Atlas simulator. The analysis is performed with an applied load of 1500 lbf and a safety factor of 2 giving a testing load of 3000 lbf in the cylinder direction onto the support beam and cylinder anchor bracket.

The resulting maximum stress of 14,000 psi is located at the cylinder anchor bracket mounting bore. The yield strength of the aluminum bracket is 40,000 psi, much higher that the resulting stress. The resulting I-beam deflection is 0.017 in, significant for a rigid support system. To resolve the deflection issue, a structural arm is added to the support structure; linking the three columns together. The analysis was repeated with the structural arm constraint in place resulting in negligible deflections. Additional analysis was performed on other components of interest. This analysis resulted in negligible stress and deflection magnitudes.

E. Orientation Measurement

Effective and reliable real-time orientation information is required for sphere control. The *Visual Orientation System* (VOS) provides low speed, absolute measurement of the sphere orientation while the *Inertial Orientation System* (IOS) measures the relative orientation of the sphere at high speed. The sensors are fused using Kalman filtering techniques yielding accurate orientation measurements used for control.

Figure 5. VOS camera and IOS.

The VOS consists of a CCD camera with a wide angle lens and a series of markers distributed over the surface of the sphere. The VOS design has been an iterative process, with considerable work undertaken on the Atlas Lite demonstrator over several years. The use of 2D barcodes was initially considered, but processing speed issues drove design development towards a simpler camera and marker system. The markers initially used three colours for identification, but concerns with the durability and scalability pushed the development of a binary marker system.

The binary markers consist of concentric circles containing a total of seven bits of information within each marker. The number represented by each marker is identified using an algorithm developed in Labview, which identifies peaks and troughs in an area between the centre and edge of the marker. It then filters the output to provide a binary signal which can be converted to an integer. Sphere orientation is determined by comparing the position of the marker identified on camera with a known marker position. The orientation of the sphere can then be geometrically determined. Due to high computational demand, the sensor is only capable of operating at 20 Hz in its current configuration.

The IOS provides sphere angular velocity data. The sensor used is a MicroStrain 3DMG device coupled to a serial to Bluetooth transmitter. The sensor is operated at 60 Hz. The IOS suffers from drift as it has no absolute reference point. This means it is not suitable for use as the sole positional sensor on the sphere. However, the information provided by the VOS is used to compensate the drift. The IOS drift compensation is accomplished by fusing the IOS and VOS, using an Unscented Kalman Filter (UKF) implemented in a C++ DLL called by Labview. The UKF updates a single predicted position with one or both of the positional inputs at an operating frequency of 60 Hz.

F. Realtime Platform Design

To achieve deterministic control of the Atlas sphere, the Atlas *Realtime Platform* (RTP) control system receives the virtual vehicle state input from the flight simulation software, and receives the physical vehicle state from sensors mounted on the sphere. It compares these inputs to calculate the error between the actual and desired sphere orientations. It then generates a command signal sent to the actuators such that the discrepancy between the virtual state and physical state is reduced below the desired tolerance of the system. The system completes the computation of the command signal in real-time, and at a sufficiently high frequency such that there is no perceptible lag to the operator of the simulator.

The control algorithm uses three independent PID controllers, each dedicated to a single sphere rotational DoF. The PID controller gains will be estimated and subsequently tuned following construction of the Atlas simulator. A detailed description of the proposed control algorithm is beyond the scope of this paper. The digital command signal from the control algorithm is sent to a Field-Programmable Gate Array (FPGA), which converts it to an analog signal. The analog command signal is sent to the three Kollmorgen servomotors, each responsible for one of the mecanum wheel actuators. The drives will be configured to operate in torque mode, and thus the input signal shall be multiplied by a programmable command gain, set using Kollmorgen proprietary configuration software connected via a serial port, to produce the desired drive current.

III. Sphere

A. Sphere Shell

Due to geometric, tooling, and cost restrictions, it was decided the sphere should be built in sections, and the panels assembled after manufacturing and delivery. Several designs for segmentation were proposed and evaluated on complexity, tooling cost, and size. It was decided that the hatches would be manufactured separately and the remainder of the sphere would be divided into four equal segments. The resulting four panel seams run from one hatch to the other, in effect dividing the sphere into slices like an orange. Figure 6 illustrates the basic segmentation of the sphere into four identical panels (hatches not shown).

The sphere panels shall have a sandwich panel design using two Epoxy-E-glass skins to carry bending loads, with a foam core to carry compressive and shear loads. The sandwich panel design greatly increases stiffness and weight savings while minimizing deflection. Fiberglass has good all-around strength characteristics and modulus. Epoxy-E-glass composite densities range from about 119 to 131 lb/ft^3, an acceptable weight range. Divinycell H is a foam core recommended by a composite manufacturer, and has a wide range of densities, strengths, and moduli allowing for design optimization.

Five composite test coupons of the desired material have been acquired. The test coupons have varying foam cores and numbers of E-glass plies as shown in Table III. The variations in lay-up will allow for the final design decision to be made after the testing has been completed on the coupons.

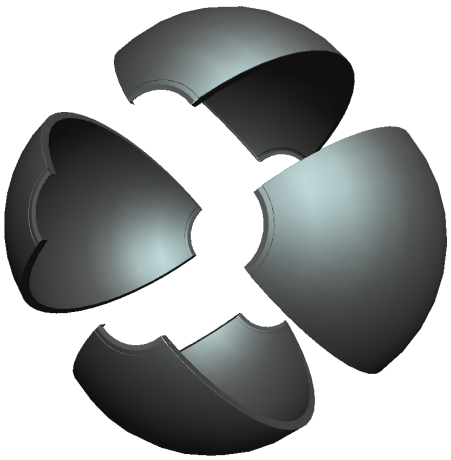

Figure 6. Segmentation of sphere panels.

TABLE III. Lay-ups of composite test panels.

Coupon	Skin 1	Foam Core	Skin 2
1	4	Divinycell H60 (5lb)	4
2	4	Divinycell H130 (8lb)	4
3	6	Divinycell H60 (5lb)	6
4	4	Divinycell H60 (5lb)	6
5	4	Divinycell H (12lb)	4

The first set of testing was completed by following ASTM D3039 and testing sample strips of the composites epoxy/E-glass skins in tension until failure. From this it was determined the laminate strength was neither orthotropic nor consistent from skin to skin. The average ultimate tensile strengths of the laminates were calculated to be under the expected value of 41,415 psi. The six ply laminate was just 2% below the expected value, though the four ply laminates were 16% under the expected. However, once the outliers were removed (from plies affected by voids and defects) the ultimate tensile strength was just 5% lower than expected.

The second set of testing was completed by following ASTM D5467 to perform four point bending tests on test strips of the sandwich panel. This allowed the determination of what deflections could be expected under given loads as well as an approximation of deflection and applied load at failure (Pmax). From comparing the results of strips (shown in Table IV) taken from test panels 1, 2, and 3, it became clear that the foam core provides the majority of the strength to the composite.

TABLE IV. Four-point bending test results.

Coupon	Plies/Skin	Foam Core	Pmax (lbf)	Deflection at Failure (in)
1	4	Divinycell H60 (5 lb)	325	0.16
1	4	Divinycell H60 (5 lb)	325	0.16
3	6	Divinycell H60 (5 lb)	375	0.18
3	6	Divinycell H60 (5 lb)	375	0.18
3	6	Divinycell H60 (5 lb)	375	0.18
2	4	Divinycell H130 (8 lb)	700	0.35
2	4	Divinycell H130 (8 lb)	700	0.35
2	4	Divinycell H130 (8 lb)	700	0.35

B. *Internal Structure*

The Atlas prototype inner structure serves to reinforce the composite panels against external forces and to rigidly mount the physical elements of the cockpit itself. Figure 7 shows three segmented parallel rings forming a frame that supports the composite panels at mid-span and reinforces the flanges at the panel edges so that custom anchor brackets can be placed to support the truss frame under the floor of the cockpit assembly. The flanges are strengthened by sheet steel stiffener plates on either side, distributing the clamping force of assembly bolts holding the panels together, see Figure 8.

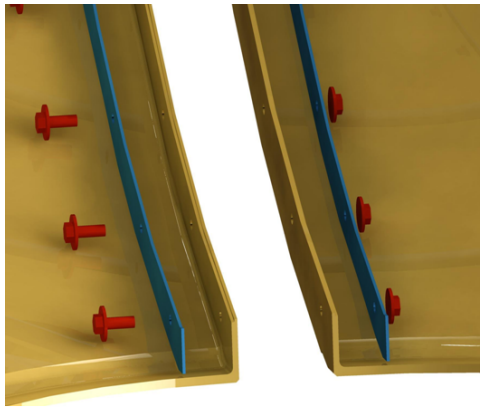

Figure 8. Flange attachment method.

Figure 7. Supporting frame.

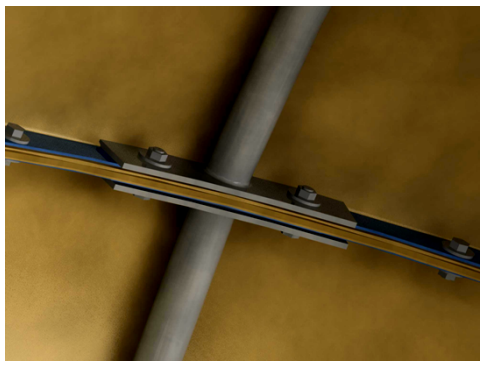

Figure 9. Rib attachment point.

The ring segments consist of 2 in diameter 6061-T6 aluminum tubing bent to match the inside curvature of the composite panels. Each segment spans the distance between the seam flanges of a single panel. Doubler plates are welded to the ends of the tubing and are bolted to the flanges by the shell assembly bolts, see Figure 9.

The cockpit floor is a bolted construction of rectangular aluminum tubing. The main beams are anchored to the reinforced shell flanges with custom made brackets and the additional frame members on either side of the pilot's chair are attached to the tubular ribs running along the bottom panel of the sphere, see Figure 10. The frame supports the pilot's chair during simulator motion and supports the full-coverage floor of the cockpit during entry and egress. The floor is designed to assemble into segments before being moved into the sphere as each segment will fit through the entry hatches after the shell has been assembled.

Classical stress analysis and finite element software have been used to confirm that the reinforcing frame will resist expected loads and that the cockpit floor frame will have the necessary strength to resist fatigue from simulator motion. Appropriate fasteners have been selected for the assembly of

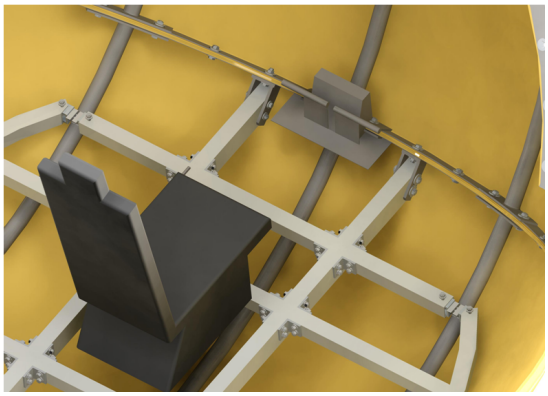

Figure 10. Floor support frame.

the sphere and its internal elements. The expected weight of the inner sphere structure and associated hardware with the current iteration of materials and dimensions is approximately 285 lb. The weight is split almost equally between the curved support ribs, the cockpit floor frame, and the flange stiffeners.

C. Hatch

To meet industry safety requirements, the design includes two easily accessible hatches on opposite poles of the sphere, see Figure 11. This ensures that, in case of an emergency, if one hatch is blocked then the occupant still has a way of getting out of the sphere quickly. The hatch design includes locking mechanism which consists of a rotating mechanism bolted to the middle part of the end cap with six cables attached to it leading to six pins surrounded by springs that keep the pins locked into grooves under the sphere panel flanges. The springs keep the hatch in place unless a force applied by the cables on to the pins compresses them to unlock the hatch. This force can be applied using a handle attached to the interior part of the rotating mechanism from inside the hatch. To release the hatch from the outside, a key that retracts the pins using the same mechanism is introduced to the hatch exterior. The hatch can then be removed using a commercially available suction cup handle.

The hatch will accommodate the required ventilation holes and hence aluminum will be used instead of composites for ease of implementation. The hatch design is 30 in in diameter with a thickness of 3/8 in. The hatch plate will have four groups of 151 holes with a diameter of 3/16 in each. Four fans will be connected to the inside of the hatch corresponding to the four groups of holes, illustrated in Figure 11. The corresponding weight of the hatch at this diameter and thickness is 36 lb. This configuration will be used to circulate air in the sphere by pushing air into one hatch and out the opposing hatch 180° across from it.

D. Internal Design and Layout

Screen based projection is the selected display method, giving users the best feeling of immersion. The specifications

Figure 11. Hatch inside and outside surfaces.

required for Atlas projection are a diagonal screen size of approximately 46 in, intensity of minimum 100 lumens and LED digital light processing technology.

Atlas is an enclosed environment and as such, lighting is needed for the safety of the occupant during emergency situations, entry and egress as well as to mimic the lighting available in a realistic cockpit environment. For adequate lighting within the sphere a minimum of 1.1 W/ft^2 of LED light strips will be provided. The LED light strips will provide two different colours for illumination within the sphere: white and red.

In selecting an appropriate battery for Atlas, consideration was given to the power budget, weight, cost and capacity. A 12 V, 52Ah Nickel Metal Hydride battery has been selected for a 1.25 hr run-time.

The layout of Atlas has been designed using anthropometric charts for a 95th percentile male (1.85 m). The major components that define the layout of the internal cockpit are: the platform, seat, pedals, screen, and joystick. The placement of the platform is governed by the need for the occupant's head to be located, at most, six inches from the geometric centre of the sphere. With these design constraints the platform must be placed approximately 0.46 m from the bottom of the sphere. The seat must be placed so that the occupant's head is within the six inch design requirement using a stationary sitting angle of 135° from the horizontal. The pedals are required to be approximately 0.56 m from the edge of the seat. Aircraft cockpit layouts traditionally place the pedals closer to the occupant than would be seen in a traditional sitting position. From this, a value of approximately 0.51 m will be used for the pedal placement. With the location of the seat determined, the screen can then be placed with respect to the occupant's head and eye position. The optimal viewing configuration is an eye-to-screen

distance of approximately 0.75-1.25 m and an eye-to-centre of screen angle of 15-20° below the horizontal, placing the screen approximately 0.50 m away from the occupant's eyes and 15° below the horizontal. The placement of the joystick takes into consideration the angle of the arm and wrist which will measure the lowest in an upper limb assessment.

IV. Simulation Software Infrastructure

In order to provide the pilot with a realistic simulation and create the highest fidelity experience possible, a sophisticated system of software infrastructure is required. This system can be simplified into two operational groups: simulation systems and the Real Time Platform.

A. CUSP Simple Infrastructure

Due to the unique design of the Atlas actuation system, wired connections for data (as well as power) are not possible between the cockpit and external computing resources. As a result, computing is distributed between internal computing resources and external computing resources to minimize required wireless network traffic and simulation cycle latency. Further, an efficient distributed computing architecture was required to facilitate software modularity. To support this, a dedicated CUSP architecture was developed.

The CUSP Simple Infrastructure (CSI) is a distributed middleware that supports federated software using a publish and subscribe communication paradigm. The CSI consists of a number of entities called 'federates'. These federates are able to assemble themselves into a group, at which point they become a federation. A special federate, called the AdminFederate, controls the assembly of individual federates into a federation, and will be present in all federations. These federations are able to exchange data between one another and are able to run across multiple computers. The key functionality the CSI provides is its publish and subscribe features. The publish feature allows any federate to 'publish' information to the rest of the CSI. Any other federates interested in receiving that information can 'subscribe' to that federate's publications in order to receive the data. This allows for a loose coupling between components in the system rather than a close relationship, and allows for a modular system design which is easily modified to satisfy future changes in the system architecture.

B. Real Time Platform

The RTP provides the simulator with a means to control the actuation of both the sphere and the Stewart platform. The RTP is comprised of two separate desktop computers running National Instruments Labview Real-time Software: one acting as an embedded system running the hard real-time control software (the RTP Target), and the host machine (the RTP host), which provides the technician with diagnostic information and control of the RTP target. The control software is designed to be completely modular and allows for the addition or removal of different components with minimal modifications. It is designed to perform the following functions: provide accurate and reliable control over sphere actuation and Stewart platform motion; CSI to receive vehicle state (VS) and fault state (FS); receive information from sensors to determine sphere absolute rotation; respond to FS's generated during operation and take actions according to the safety system design.

V. Conclusion

This paper has presented aspects of the detail design of the first full scale Atlas motion platform prototype, a novel six DOF motion platform with decoupled positioning and orienting capabilities. The workspace is free from configurational and representational singularities, and the orienting workspace is unbounded. This compelling attribute can be exploited to provide motion platforms for a wide range of applications. The motions of virtually any vehicle can be replicated. While the Atlas platform offers potential significant advantages in terms of range of motion, several practical technical challenges needed to be addressed. The actuation system has been sized and selected. Design challenges regarding the actuation system, the sphere structure, and simulation software were resolved and presented herein publicly for the first time.

References

[1] M. J. D. Hayes and R. G. Langlois, "Atlas: a Novel Kinematic Architecture for Six DOF Motion Platforms," Transaction of the Canadian Society for Mechanical Engineering, vol. 29 (4), 2005, pp. 701–709.

[2] V. E. Gough, "Discussion in London: Automobile Stability, Control, and Tyre Performance," Proc. Automobile Division, Institution of Mech. Engrs., 1956, pp. 392–394.

[3] D. Stewart, "A Platform With Six Degrees of Freedom," Proc. Instn. Mech. Engr., vol. 180 (15), 1965, pp. 371–378.

[4] F. Williams, E. R. Laithwaite, and G. F. Eastham, "Development and Design of Spherical Induction Motors," Proc. IEEE, vol. 47, 1959, pp. 471–484.

[5] R. B. Roth and K.-M. Lee, "Design Optimization of a Three-Degree-of-Freedom Variable Reluctance Spherical Wrist Motor," ASME J. Eng. Industry, vol. 117, 1995, pp. 378–388.

[6] G. S. Chirikjian and D. Stein, "Kinematic Design and Commutation of a Spherical Stepper Motor," IEEE/ASME Transactions on Mechatronics, vol. 4 (4), 1965, pp. 342–353.

[7] J. Kim, J.-C. Hwang, J.-S. Kim, C. Iurascu, F. C. Park, and Y. M. Cho, "Eclipse-11: a New Parallel Mechanism Enabling Continuous 360-Degree Spinning Plus Three-axis Translational Motions," IEEE Transactions on Robotics and Automation, vol. 18 (3), 2002, pp. 367–373.

[8] W. Bles and E. Groen, "The DESDEMONA Motion Facility: Applications for Space Research," Microgravity Science and Technology, vol. 21 (4), 2009, pp. 281–286.

[9] M. J. D. Hayes, R. G. Langlois, and A. Weiss, "Atlas Motion Platform Generalized Kinematic Model," Meccanica, vol. 46 (1), 2011, pp. 17–25.

[10] R. Ahmad, P. Toonders, M. J. D. Hayes, and R. G. Langlois, "Atlas Mecanum Wheel Jacobian Empirical Validation," in Proc. of The Can. Soc. for Mech. Eng. International Congress, 2012, on CD.